levels[4]. The classical capacitance really corresponds to the *flat-band* limit. Also, it may be noted that quantum capacitance involves a change of the chemical potential with change in the electron density and is, therefore, related to the compressibility of the electron gas. In a real system with electron–electron and electron–ion interactions, however, one would expect corrections to (renormalization of) the free-electron gas value calculated here. Finally, a technical remark. The present calculation refers to the direct capacitance between two conductors in isolation. In general, however, the charging energies of a system of conductors, with or without a common *ground*, is a bilinear expression in the charges residing on the conductors, with a *coefficients-of-capacitance* matrix that determines the self- and the mutual capacitances, known as the capacity coefficients (diagonal) and the electrostatic induction coefficients (off-diagonal), respectively[5]. Our quantum capacitance forms part of the self-capacitance. The calculation refers to the simplest case of just two oppositely charged identical conductors forming a planar or bifilar capacitor – an operationally well-defined situation.

1. Missert, N. and Beasley, M. R., *Phys. Rev. Lett.*, 1989, **63**, 672; Triscone, J. -M., Fisher, O., Brunner, O., Antognaza, L., Kent, A. D. and Karkut, M. G., *Phys. Rev. Lett.*, 1990, **64**, 804.
2. Heinrich, H., Bauer, G. and Kuchar, F. (eds), *Physics and Technology of Sub-micron Structures*, Springer Series in Solid-State Science, vol. 83; Weisbuch, C. and Vinter, B., *Quantum Semiconductor Structures*, Academic Press, London, 1991.
3. Likharev, K. K., *IBM J. Res. Develop.*, 1988, **32**, 144.
4. Eaves, L., in *Analogies in Optics and Micro Electronics*, (eds Haeringen, W. van. and Lenstra, D.), Kluwer, London, 1990, p. 227.
5. Landau, L. D. and Lifshitz, E. M., *Electrodynamics of Continuous Media*, Pergamon, Oxford, 1966.

Received 30 January 1995; revised accepted 11 April 1995

Lyapunov exponents and predictability of the tropical coupled ocean–atmosphere system

A. Anantha Raman, B. N. Goswami* and A. Chandrasekar†

Department of Physics and Meteorology, Indian Institute of Technology, Kharagpur 721 302, India
*Centre for Atmospheric Sciences, Indian Institute of Science, Bangalore 560 012, India

It has recently been proposed that the broad spectrum of interannual variability in the tropics with a peak around four years results from an interaction between the linear low-frequency oscillatory mode of the coupled system and the nonlinear higher-frequency modes of the system. In this study we determine the Lyapunov exponents of the conceptual model consisting of a nonlinear low-order model coupled to a linear oscillator for various values of the coupling constants.

TODAY even with sophisticated computing, complex general circulation models and experimental resources available, we cannot predict accurately the state of the atmosphere. This is due to the existence of an upper limit on deterministic predictability of the atmosphere. The reasons for the upper limit are that the equations governing the atmosphere are nonlinear and the atmosphere is characterized by both horizontal and vertical gradients of wind, temperature and moisture, which permit hydrodynamical and thermodynamical instabilities to grow. The quantitative upper limit for deterministic prediction is determined by the growth rates and equilibration of the most dominant instabilities.

The phenomenon of sensitive dependence on initial conditions, known as chaos, means that two trajectories initially separated by a small value may get vastly separated after some time. The Lyapunov exponents measure quantities which constitute the exponential divergence or convergence of nearby initial points in the phase space of a dynamical system. Thus, when sensitive dependence on initial conditions leads to divergent trajectories and, consequently, loss of information, we can quantify the rate at which the information is lost through these exponents. Lyapunov exponents of a dynamical system are one of the invariants that characterize the 'attractors' of the system. Attractors can be thought of as a distribution of points in a phase or state space characterized by the density of points. The Lyapunov exponents are independent of the initial conditions on any orbit and thus are properties of the attractor geometry and the dynamics[1]. A positive Lyapunov exponent measures the average exponential divergence of two nearby trajectories whereas a negative exponent measures the exponential convergence of two nearby trajectories[2]. Thus, a positive Lyapunov exponent may be taken as a manifestation of chaos.

Recently, a number of studies on the predictability of the atmosphere using coupled ocean atmospheric systems have been reported in the literature[3–5]. Goswami and Shukla[4] used classical predictability methods to arrive at two distinct time scales for growth of small

†For correspondence.

errors. The slow time scale provides a basis for long-range predictability and appears to arise as a result of a dominant four-year cycle of the system, while the fast time scale appears to arise due to the aperiodicity of the system. Krishnamurthy, Goswami and Legnani[6] have recently proposed a conceptual model for the aperiodicity of the interannual variability of the tropics. The model consists of a nonlinear system (Lorenz model[7]) coupled to a linear oscillator. The nonlinear system represents some aspects of the general circulation of the atmosphere and the equations are the same as those of Lorenz[7]. The linear part represents the dominant four-year oscillation of the coupled system arising due to unstable air–sea interactions in the tropics and reflection of Rossby waves from the western boundary[8]. Due to the very large horizontal scale involved, the equatorial Rossby number for this phenomenon is small and hence may be considered linear.

The conceptual model may be written as

$$\dot{X} = -Y^2 - Z^2 - aX + aF, \tag{1}$$

$$\dot{Y} = XY - bXZ - cY + G + \alpha P, \tag{2}$$

$$\dot{Z} = bXY + XZ - cZ + \alpha Q, \tag{3}$$

$$\dot{P} = -\omega Q - \beta Y, \tag{4}$$

$$\dot{Q} = \omega P - \beta Z, \tag{5}$$

where ω is the frequency of the low-frequency oscillator with a period of four years, P and Q are the amplitudes of the sine and cosine phases of the oscillation and α and β are the coupling strengths. The above nonlinear system [eqs (1)–(3)] is obtained by rescaling the Lorentz system by a factor c as (original values are denoted by primes)

$$t = t'/c;\ X = cX';\ Y = cY';\ Z = cZ',$$

$$a = a'c;\ b = b';\ F = cF';\ G = c^2 G'.$$

X may be interpreted as a zonally averaged field while Y and Z may be interpreted as amplitudes of the two wave components. F is interpreted as external zonally symmetric forcing (e.g. solar forcing) while G is the zonally asymmetric forcing (e.g. land–ocean contrast). We have used $c = 0.5$ and have retained the same values of the unscaled coefficients $a = 0.25$ and $b = 4$ as used by Lorenz.

The method used in this study is based on the algorithm of Wolf *et al.*[9] for the calculation of the Lyapunov exponents from a set of differential equations. As a test of the code, the Lyapunov exponents for the Lorenz convection model[10] as given in Wolf *et al.*[9] were calculated and had values $\lambda_1 = 2.1643$, $\lambda_2 = 1.6967 \times 10^{-6}$ and $\lambda_3 = -32.50$. The accepted values of the exponents for the Lorenz equations as mentioned in Wolf *et al.*[9] are $\lambda_1 = 2.16$, $\lambda_2 = 0.0$ and $\lambda_3 = -32.40$.

Having tested the algorithm by computing the exponents for the Lorenz model, we evaluated the same for the conceptual model [eqs (1)–(5)]. Table 1 provides the values of the five exponents for a coupled case ($\alpha = \beta = 0.05$) and for various values of F (6, 7, 8, 9) and G (0.125, 0.25, 0.50). The convergence of the exponents was checked using the criterion

$$|\lambda_i^{k+1} - \lambda_i^k| < \sigma\,|\lambda_i^k|, \quad i = 1, 2, 3, 4, 5. \tag{6}$$

The superscript k indicates the index for the march of the integration. It was found that for $\sigma = 10^{-5}$, the number of integration marchings required for all the various cases were of the order of one lakh or less (the time step was one-eighth of a day). All the calculations were carried out in double precision. Consideration of computer time as well as the need for accurate values of the Lyapunov exponents led us to enforce the following criterion. The integrations were terminated when either the criterion in eq. (6) with $\sigma = 10^{-6}$ was satisfied or when the number of integration marchings reached a value of 6 lakhs. Since F refers to external forcings such as solar insolation, which also

Table 1. Lyapunov exponents for $\alpha = \beta = 0.05$ and for different values of F and G

F, G	λ_1	λ_2	λ_3	λ_4	λ_5
6, 0.125	2.17×10^{-6}	-1.57×10^{-4}	-1.59×10^{-4}	-2.37×10^{-3}	-2.41×10^{-3}
7, 0.125	1.43×10^{-4}	1.52×10^{-5}	2.12×10^{-6}	-1.29×10^{-4}	-4.09×10^{-3}
8, 0.125	2.64×10^{-4}	6.13×10^{-5}	1.40×10^{-6}	-5.63×10^{-5}	-4.69×10^{-3}
9, 0.125	8.43×10^{-4}	2.60×10^{-5}	3.23×10^{-6}	-1.03×10^{-4}	-5.36×10^{-3}
6, 0.25	-4.52×10^{-6}	-1.20×10^{-4}	-1.27×10^{-4}	-1.26×10^{-3}	-1.00×10^{-2}
7, 0.25	1.02×10^{-4}	-5.55×10^{-5}	-6.98×10^{-5}	-3.06×10^{-4}	-7.20×10^{-3}
8, 0.25	8.83×10^{-6}	-6.62×10^{-5}	-7.87×10^{-5}	-2.66×10^{-3}	-2.88×10^{-3}
9, 0.25	5.41×10^{-6}	-1.21×10^{-4}	-1.20×10^{-4}	-1.48×10^{-3}	-1.52×10^{-3}
6, 0.5	-1.37×10^{-5}	-6.22×10^{-5}	-4.97×10^{-3}	-5.01×10^{-3}	-3.22×10^{-2}
7, 0.5	-5.75×10^{-5}	-9.47×10^{-5}	-8.44×10^{-3}	-8.47×10^{-3}	-2.39×10–2
8, 0.5	1.17×10^{-3}	-4.50×10^{-6}	-4.14×10^{-3}	-5.09×10^{-3}	-1.81×10^{-2}
9, 0.5	3.63×10^{-6}	-1.00×10^{-3}	-1.59×10^{-3}	-1.36×10^{-2}	-1.81×10^{-2}

changes with time around a year, we have evaluated the exponents for different values of F. It is clear from Table 1 that for all the four values of F (6, 7, 8, 9) and for $G = 0.125$, the system is chaotic. The same, however, cannot be said for the values of $F = 6$ and $G = 0.25$ as well as $F = 6$ and 7 and $G = 0.5$. It is also seen from Table 1 that the increase in the value of F for a fixed value of G causes more modes with positive Lyapunov exponents to appear. Since G refers to asymmetric forcings, we also wished to examine the behaviour of the system with a different value of G (0.125, 0.25, 0.5). It is evident from Table 1 that an increase in the value of G for a fixed value of F gives rise to a situation where chaos is absent. This is especially evident for case of $F = 6$ when G increases from 0.125 to 0.5. This is to be expected as it is known from the Lorenz model that for such large values of G the model has a periodic orbit. The above results where more modes with positive Lyapunov exponents manifest for small values of G and large values of F seem consistent with Lorenz's observation that the behaviour of the atmosphere is analogous to his model with large F and small values of G.

The coupling of the nonlinear system with the linear oscillator is accomplished using the coupling constants α and β. Table 2 presents the values of the five exponents for $F = 7$ and $G = 0.125$ and for different values of α (0, 0.05, 0.1) and β (0.0, 0.05, 0.1). One would expect that for the uncoupled case ($\alpha = \beta = 0.0$) atmospheric chaos will prevail. This is evident from the appearance of a positive exponent in Table 2. With the introduction of coupling ($\alpha = 0.0$; $\beta = 0.05$ and 0.1), it is seen that more modes appear with positive exponents. This is consistent as nonzero β value introduces a low-frequency component. The effect of increasing α from 0 to 0.1 for $\beta = 0$ causes all exponents to be negative. For the cases of $\alpha = 0$, $\beta = 0.05$ and $\alpha = 0$; $\beta = 0.1$ it was found that the number of integration marchings required were of the order of one crore. However, it turned out that for the cases of $\beta = 0$, $\alpha = 0$, $\beta = 0$, $\alpha = 0.05$ and $\beta = 0$, $\alpha = 0.1$ the fourth and fifth exponents assumed a value very close to zero (of the order of 10^{-18}), thereby assuming a value higher in magnitude compared to the second and third exponents.

It was felt that a better way of illustrating the variation of the Lyapunov exponents with system parameters like coupling strengths and strengths of the forcing was through figures. Figures 1–4 depict the variation of Lyapunov exponents with forcings (F and G) and with coupling strengths (β and α). The data for the figures were taken from Tables 1 and 2, respectively. A line is drawn in these figures (for convenience) connecting the values of the exponents; the numbers 1–5 in the figures denote the exponents (λ_1–λ_5).

In order to deduce the possible role of the particular value of ω (4 years), it was decided to run a couple of experiments with different values of ω (2 and 7 years) for $F = 7$, $G = 0.125$, $\alpha = \beta = 0.05$. It is known that the broad spectrum of interannual variability in the tropics has a peak in the range of 2–7 years and, therefore, the above values of ω were chosen. It was found that the system remained chaotic for $\omega = 2$ and 7 years. However, the number of positive exponents were two for $\omega = 2$ years and one for $\omega = 7$ years.

For systems whose equations of motion are explicitly known determination of the complete Lyapunov spectrum is relatively straightforward. The Lyapunov exponents may be defined by the phase space evolution of a sphere of states. However, efforts to apply this definition numerically to equations of motion fail since computer limitations do not allow the initial sphere to be constructed sufficiently small. This problem is avoided with the use of a phase space plus tangent space approach so that one obtains always infinitesimal principal axis vectors. The remaining divergences of the orthonormal vectors are overcome by repeated use of the Gram Schmidt reorthonormalization (GSR) procedure on the vector frame. Thus, repeated use of GSR allows the integration of the vector frame for as long as required for spectral convergence. We feel that the calculations carried out in double precision with sufficient integration marchings should yield robust values of the Lyapunov exponents. Since the Lyapunov exponents change in general if the

Table 2. Lyapunov exponents for $F = 7.0$, $G = 0.125$ and for different values of α and β

α, β	λ_1	λ_2	λ_3	λ_4	λ_5
0, 0	1.96×10^{-6}	-1.82×10^{-3}	-1.82×10^{-3}	0.0	0.0
0, 0.05	2.59×10^{-9}	9.80×10^{-11}	-3.37×10^{-13}	-9.12×10^{-4}	-9.12×10^{-4}
0, 0.1	2.34×10^{-9}	3.53×10^{-10}	-1.35×10^{-12}	-9.12×10^{-4}	-9.12×10^{-4}
0.05, 0	1.14×10^{-6}	-1.57×10^{-3}	-2.04×10^{-3}	0.0	0.0
0.05, 0.05	1.43×10^{-4}	1.52×10^{-5}	2.12×10^{-6}	-1.29×10^{-4}	-4.09×10^{-3}
0.05, 0.1	7.57×10^{-6}	-2.28×10^{-6}	-1.29×10^{-4}	-1.58×10^{-4}	-3.42×10^{-3}
0.1, 0	-4.35×10^{-7}	-9.89×10^{-5}	-3.45×10^{-3}	0.0	0.0
0.1, 0.05	5.77×10^{-6}	2.01×10^{-6}	-1.11×10^{-4}	-1.72×10^{-4}	-3.43×10^{-3}
0.1, 0.1	7.68×10^{-6}	-6.59×10^{-4}	-6.60×10^{-4}	-1.37×10^{-3}	-1.41×10^{-3}

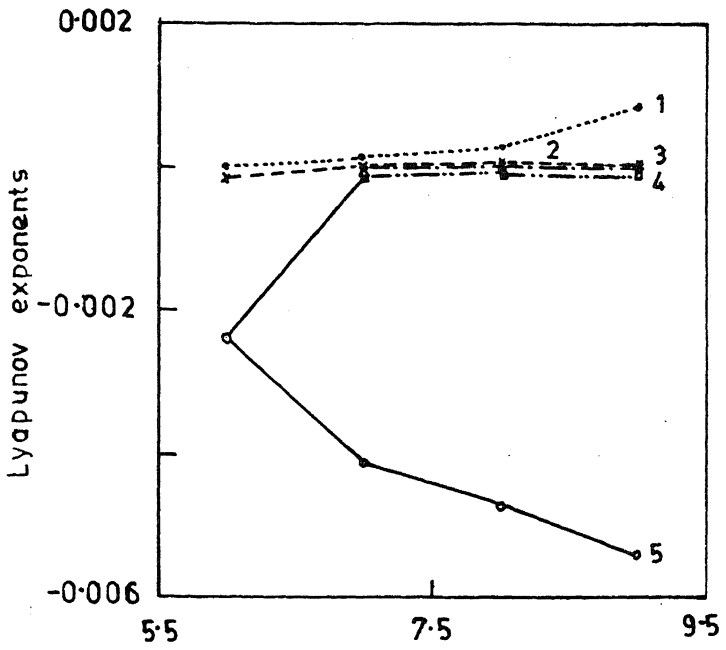

Figure 1. Variation of the Lyapunov exponents with F for $\alpha = \beta = 0.05$ and $G = 0.125$.

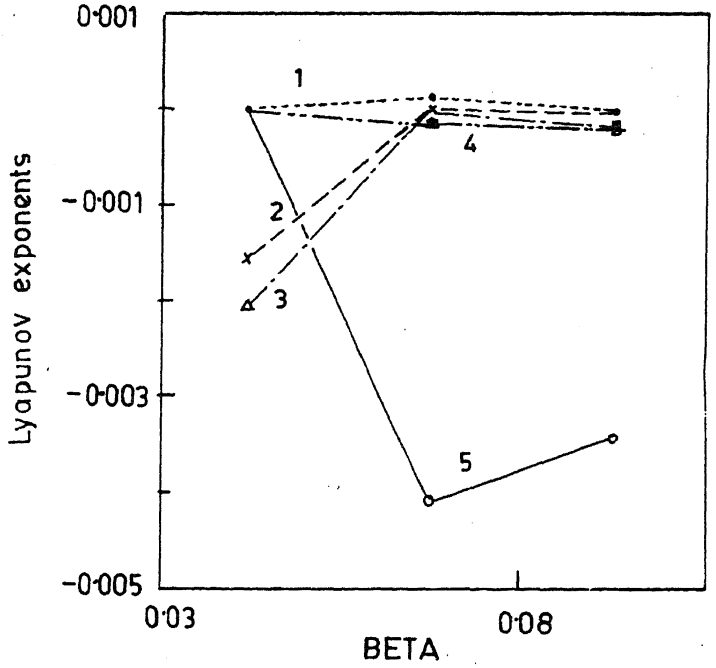

Figure 3. Variation of the Lyapunov exponents with β for $\alpha = 0.05$, $F = 7.0$ and $G = 0.125$.

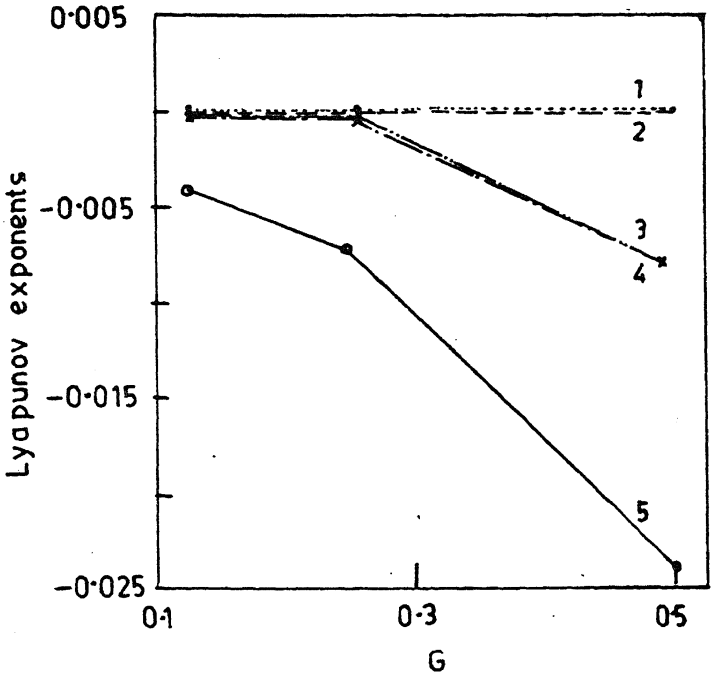

Figure 2. Variation of the Lyapunov exponents with G for $\alpha = \beta = 0.05$ and $F = 7.0$.

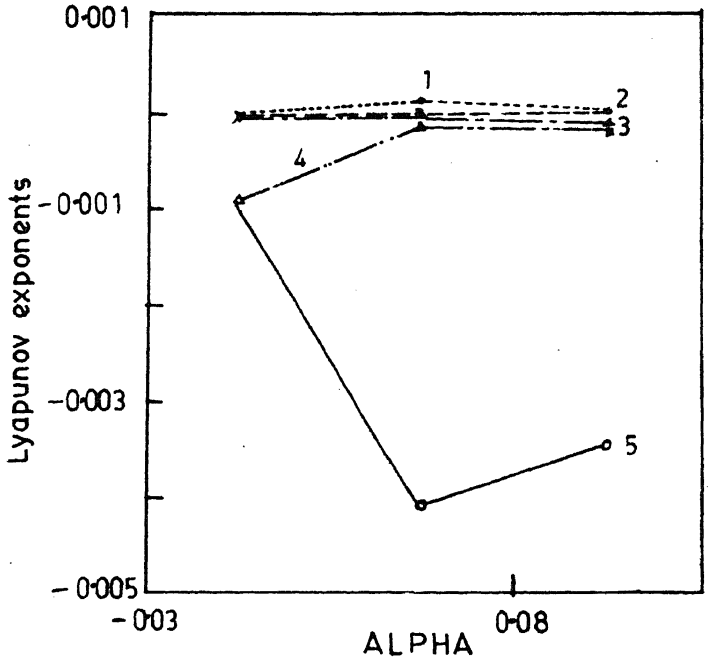

Figure 4. Variation of the Lyapunov exponents with α for $\beta = 0.05$, $F = 7.0$ and $G = 0.125$.

forcing values are changed, we have examined the system with varying values of forcing. This is akin to looking at the behaviour of the system at different periods of the year, where one may assume that the values of the forcing are more or less constant within each of the individual periods. We have obtained the result that for some values of F and G the computed exponents are positive while for some others they are negative. The interesting consequence of such a result is that if the model imitates the behaviour of the coupled ocean–atmosphere system, then the system is not always chaotic but, in fact, becomes one for some conditions which are controlled by the forcings. Thus, if we examine the coupled system behaviour over a period of one year (the same being the periodicity of the forcings), then the system is stable for some parts of the year while for some other it behaves chaotically. This is exactly the cause of the unpredictability of the atmosphere. There is evidence[4] that the tropical coupled system is most unpredictable during boreal spring and most predictable during boreal winter. Even though for part of the forcing period (e.g. part of the annual cycle) the system is not chaotic and may be predictable, when it passes through the period of the forcing where it is

chaotic, any two nearby similar trajectories are thrown apart. This introduces loss of predictability even for the low-frequency component.

1. Blumenthal, M. B. and Paul Bryant, *Phys. Rev. A*, 1991, **43**, 2787–2806.
2. Gencay, R. and Dechert, W. D., *Physica D*, 1992, **59**, 142–157.
3. Blumenthal, M. B., *J. Climate*, 1991, **4**, 766–784.
4. Goswami, B. N. and Shukla, J., *J. Climate*, 1991, **4**, 3–21.
5. Goswami, B. N. and Shukla, J., *J. Climate*, 1993, **6**, 628–638.
6. Krishnamurthy, V., Goswami, B. N. and Legnani, R., *Geophys. Res. Lett.*, 1993, **20**, 435–438.
7. Lorenz, E. N., *Tellus*, 1984, **36A**, 98–110.
8. Suarez, M. J. and Schopf, P. S., *J. Atmos. Sci.*, 1988, **45**, 3283–3287.
9. Wolf, A., Swift, J. B., Swinny, H. L. and Vastano, J. A., *Physica D*, 1985, **16**, 285–317.
10. Lorenz, E. N., *J. Atmos. Sci.*, 1963, **20**, 130–141.

Received 15 September 1994; revised accepted 16 February 1995

Possibility of usage of return maps to predict dynamical behaviour of lakes: Hypothetical approach

B. S. Daya Sagar and B. S. Prakasa Rao
Centre for Remote Sensing, Department of Geo-Engineering, Andhra University, Visakhapatnam 530 003, India

In this article, we show how one-dimensional maps can be useful in analysing experimentally the dynamics of lake systems. We illustrate this by means of hypothetical lake systems.

ONE of the ways to make a complex system easier to analyse is by reducing the system to a simple system that still captures the important features of the original system. As the theory of one-dimensional (1-D) maps is well developed in several fields[1–4], it will be useful if an appropriate 1-D map can be constructed from the system under study. In this communication, we demonstrate how an approximate 1-D map can be used to analyse the dynamical behaviour of some simulated hypothetical lakes. The first-order difference equations and the general conditions of the water bodies, and the logistic map analysis for various possibilities are hypothetically described in successive sections.

A treatise by May[1] lucidly explained the role of the first-order difference equations, dynamical properties and bifurcation generations in the application of 'simple mathematical models with very complicated dynamical systems'.

The difference equation can be used for studying a dynamical system as a water body at different time intervals. It is represented as

$$X_{t+1} = F(X_t), \tag{1}$$

where X_t and X_{t+1} are the populations (pixel population in water body) of a natural system at time periods t and $t+1$, respectively. It indicates that output becomes an input feedback, and hence an iterative process. The following expression shows the relation between X_t and X_{t+1}:

$$X_{t+2} = F(X_{t+1}). \tag{2}$$

The magnitude of population at a definite time in a natural system is related to the magnitude of the population in the preceding generation. This can be represented applying the first-order difference equation $X_{t+1} = \lambda X_t(1 - X_t)$, or $X_{t+1} = \lambda X_t - \lambda X_t^2$, in which the first term is linear and the second nonlinear. In this equation the term λ will give an idea about the magnitude of variation. This equation defines an inverted parabola with intercepts at $X_t = 0$ and 1, and a maximum value of $X_{t+1} = \lambda/4$ at $X_t = 0.5$. If $\lambda > 1$, it is an indication that the population growth rate is increasing. The parameter λ gives the entire description of the system. The steepness of the inverted parabola in the logistic map depends on λ. If $\lambda < 1$, the population death rate is said to be increasing. The strength of nonlinearity explains the temporal changes in the dynamical system. Till a certain degree of magnitude of nonlinearity, the growth in areal extent of the water body will be attracted to the equilibrium stage specific to that level of nonlinearity. For a magnitude range $\lambda = 3.57$–4, the dynamical system shows chaotic behaviour, revealing that the areal extent of the water body is repelling. All the parameters in the difference equation should be such as to fix the linear term to between 0 and 1, and the strength of nonlinearity[1] to between 0 and 4, failing which the areal extent tends to become extinct. The graphic analysis explains that the normalized status of a dynamical system as water body if starting at larger than 1, it immediately goes negative and becomes extinct at one time step. Moreover, if $\lambda > 4$, the hump of the parabola exceeds 1, thus enabling the initial population near 0.5 to become extinct in two time steps. Therefore, there is a need to restrict the analysis[1] to values of λ between 1 and 4 and values of X_0 between 0 and 1. As the areal extent X_0 of the water body is small (much less than 1 on a normalized scale, where 1 might stand for any number such as 1 million km^2), the nonlinear term can initially be neglected. Then the areal extent at time step (year) $t = 1$ will be approximately equal to λX_0. Figure 1 shows a logistic model and its essential